

Disorder and size effects in the envelope-function approximation

T. G. Dargam, R. B. Capaz, and Belita Koiller

Instituto de Física, Universidade Federal do Rio de Janeiro, Caixa Postal 68.528, Rio de Janeiro, 21945-970, Brazil

(Received 19 March 1997)

We investigate the validity and limitations of the envelope-function approximation (EFA), widely accepted for the description of the electronic states of semiconductor heterostructures. We consider narrow quantum wells of GaAs confined by $\text{Al}_x\text{Ga}_{1-x}\text{As}$ barriers. Calculations performed within the tight-binding approximation using ensembles of supercells are compared to the EFA results. Results for miniband widths in superlattices obtained in different approximations are also discussed. The main source of discrepancy for narrow wells is the treatment of alloy disorder within the virtual crystal approximation. We also test the two key assumptions of the EFA: (a) that the electronic wave functions have Bloch symmetry with well-defined \vec{k} in the alloy region; (b) that the periodic parts of the Bloch functions are the same throughout the heterostructure. We show that inaccuracies are mainly due to the former assumption. [S0163-1829(97)03939-8]

I. INTRODUCTION

The proposal and demonstration of quantum effects in two-dimensional semiconductor heterostructures led to increased interest and significant progress in semiconductor experimental and theoretical techniques. From the experimental point of view, material improvement and powerful multilayer growth systems were developed, allowing monolayer-precision fabrication. The theoretical description of these translation-symmetry-broken heterostructures motivated the development of novel formalisms. The most successful and widely adopted theoretical approach for the electronic structure of these systems is the envelope-function approximation (EFA), developed by Bastard and collaborators.¹

The EFA for a model heterostructure with abrupt interfaces relies in a number of approximations. Within each layer, the wave function is written as an expansion over different bands ℓ on the periodic part of Bloch functions of well defined \vec{k} , an assumption that needs to be justified for alloys. Another key assumption is that the periodic part of the Bloch function, $u_k^\ell(\vec{r})$, is the same for each band of the different materials which constitute the heterostructure. The electronic wave functions are expanded in terms of the u 's, and the assumed translational invariance of the problem along the planes perpendicular to the growth axis (z axis) leads to a factorization of the expansion coefficients into a plane-wave \vec{k}_\perp part and a z -dependent term. The z -dependent term of the expansion coefficients, $\phi(z)$, is called the *envelope function*.

The simplest situation is to assume that the heterostructure states may be obtained from a single isotropic parabolic band for each host material. Different host materials are thus characterized by the respective effective masses and band-edge energies. The envelope function satisfies a one-dimensional Schrödinger-like equation²

$$\left[-\frac{\hbar^2}{2} \frac{\partial}{\partial z} \frac{1}{m^*(z)} \frac{\partial}{\partial z} + V(z) \right] \phi(z) = E \phi(z), \quad (1)$$

where we take $\vec{k}_\perp = 0$. In the envelope function scheme, the presence of different materials along the z direction reflects in the electrons as if they moved through a continuous medium with variable effective mass $m^*(z)$ and subject to an external potential $V(z)$. The form of Eq. (1) implies that across an interface the matching conditions² are the continuity of $\phi(z)$ and of $1/m^*(z) \partial \phi(z) / \partial z$. This point has been questioned in the literature.³

In the design of heterostructures for specific realizations, one or more of the materials involved are alloys of elemental or binary semiconductors. The alloy region in the EFA is treated within the virtual crystal approximation (VCA). The VCA recovers the translational symmetry of the potential in a disordered alloy by replacing the atoms by "averaged" ones. The other assumptions of the EFA, such as expansions in terms of Bloch functions and effective masses, are readily implemented within the VCA. In the present work we investigate several aspects of the EFA by contrasting electronic structure calculations for bulk alloys, single quantum wells, and superlattices performed both within the EFA/VCA and the tight-binding approximation. The materials considered are GaAs and direct-gap $\text{Al}_x\text{Ga}_{1-x}\text{As}$ ($x < 0.4$), so that the isotropic single-band assumption leading to Eq. (1) is in principle justifiable for the conduction-band electron states. The tight-binding approximation allows an atomic-scale description of the different materials, therefore the discrete nature of the crystal potential is preserved. In contrast with the continuous-medium assumptions in the EFA [e.g., effective masses, $V(z)$], discrepancies are expected for narrow wells.⁴ The tight-binding supercell formalism also allows a realistic treatment of the disorder in the alloy region.⁵ For comparison, tight-binding calculations within the VCA are also performed. We adopt the sp^3s^* parametrization of Vogl *et al.*⁶ in all tight-binding calculations. In Sec. II we consider $\text{Al}_x\text{Ga}_{1-x}\text{As}$ bulk alloys. The amount of zinc-blende \vec{k} symmetry in the random alloy wave functions is investigated through their spectral decomposition. The EFA assumption concerning the periodic part of Bloch functions in different materials is also investigated. In Sec. III, GaAs/ $\text{Al}_x\text{Ga}_{1-x}\text{As}$

quantum wells and superlattices are studied, and in Sec. IV we present our discussions and conclusions.

II. BLOCH-LIKE CHARACTER OF ALLOY WAVE FUNCTIONS

The first aspect within the EFA we investigate is the formal validity of the Bloch function description within the alloy region. $\text{Al}_x\text{Ga}_{1-x}\text{As}$ alloys are characterized by a critical concentration x_c that determines the crossover from a direct band-gap semiconductor ($x < x_c$) to an indirect band-gap semiconductor ($x > x_c$). The usual criterion for this transition described in the literature relies on the VCA: Although an alloy has no translational invariance, zinc-blende symmetry is recovered within the VCA. For $\text{Al}_x\text{Ga}_{1-x}\text{As}$, the crystal potential is approximated by

$$U_{\text{VCA}}(\vec{r}) = xU_{\text{AlAs}}(\vec{r}) + (1-x)U_{\text{GaAs}}(\vec{r}), \quad (2)$$

which is periodic. Within VCA, the top of the valence band is always a Γ point and the direct-to-indirect crossover is identified with a Γ -X transition in the conduction-band wave function symmetry. Using finite-size scaling techniques in supercells, Koiller and Capaz⁵ have recently shown that this crossover is analogous to a first-order phase transition, in the sense that it produces a discontinuous change in some ‘‘order parameter.’’⁷ This result, which was obtained using only real-space techniques, is consistent with a VCA-type of transition (Γ -X crossing in reciprocal space). Disorder, however, prevents an alloy wave function from having *purely* Γ or X symmetry. Therefore, to verify the consistency with the EFA assumptions, the reciprocal-space meaning of Koiller and Capaz results should be understood.

We perform a Fourier analysis of the band-edge wave functions of both direct and indirect gap structures in a large (16 000 atoms) fcc supercell. The supercell consists of $20 \times 20 \times 20$ fcc primitive cells of the zinc-blende structure. The real-space wave functions in the tight-binding approach

$$\Psi_{\text{TB}} = \sum_{\alpha, \vec{R}} c_{\alpha}(\vec{R}) |\alpha, \vec{R}\rangle \quad (3)$$

are defined by their expansion coefficients $c_{\alpha}(\vec{R})$ in the atomic orbital α ($\alpha = s, p_x, p_y, p_z, s^*$) and zinc-blende site \vec{R} . These coefficients are periodic in the supercell and therefore can be expressed as Fourier sums,

$$c_{\alpha}(\vec{R}) = \frac{1}{\sqrt{N}} \sum_{\vec{k}} e^{-i\vec{k} \cdot \vec{R}} c_{\alpha}(\vec{k}), \quad (4)$$

where the wave vectors in the sum are only those allowed by periodic boundary conditions in the supercell. These wave vectors define a $20 \times 20 \times 20$ grid in the Brillouin zone. We then define an orbital-averaged ‘‘spectral weight’’ as

$$W(\vec{k}) = \sum_{\alpha} |c_{\alpha}(\vec{k})|^2 = \frac{1}{N} \sum_{\alpha, \vec{R}, \vec{R}'} e^{i\vec{k} \cdot (\vec{R} - \vec{R}')} c_{\alpha}(\vec{R}) c_{\alpha}^*(\vec{R}'), \quad (5)$$

which quantifies the amount of zinc-blende \vec{k} -symmetry character in the wave functions.

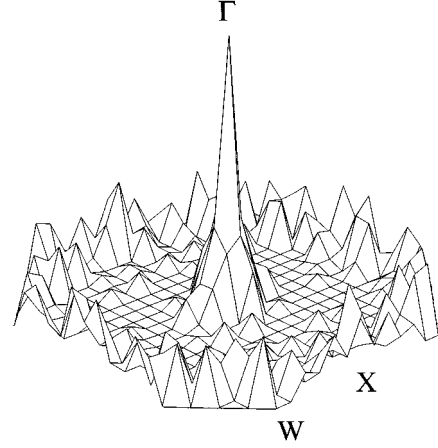


FIG. 1. Logarithm of the spectral weight $\ln W(\vec{k})$ in the plane $k_z = 0$. The plot scale varies from a minimum of -11 to a maximum of -0.64 for the state at the bottom of the conduction band of a direct-gap alloy.

In Fig. 1 we plot $W(\vec{k})$ in a logarithmic scale in the plane $k_z = 0$. It represents the spectral weight of the wave function in the bottom of the conduction band for a direct-gap structure with x slightly below x_c . The Γ point retains considerable spectral weight (53%). The remaining weight spreads over the whole Brillouin zone, particularly around the edges, a disorder effect that cannot be obtained within VCA. For indirect-gap structures the situation changes drastically and the conduction-band wave functions have typically less than 0.1% weight at Γ .

In what follows, we restrict the Al concentration in the alloy regions of heterostructures to values considerably below x_c , which means the Γ symmetry of the conduction-band edge state in the *bulk alloy* is reasonably preserved. For $x = 0.2$ (0.3), the spectral weight at Γ for the conduction-band edge is above 85% (75%). These numbers give an estimate of the error involved when, within the EFA, the bottom of the conduction-band state in $\text{Al}_x\text{Ga}_{1-x}\text{As}$ direct-gap alloys is approximated by its normalized $\vec{k} = \Gamma$ component alone: $\Psi_{\text{alloy}} \approx |\Gamma\rangle$. We conclude that this procedure is not quantitatively accurate, but may be reasonably justified for alloys with low Al concentration.

We also investigate the validity of the second EFA assumption — that the periodic part $u_{\vec{k}}(\vec{r})$ of the Bloch function is the same for each band of different materials which constitute the heterostructure. For the bottom of the conduction-band state in $\text{GaAs}/\text{Al}_x\text{Ga}_{1-x}\text{As}$ heterostructures, the alloy normalized $|\Gamma\rangle$ component should be compared to the GaAs corresponding Γ state. We find the projection $\langle \Gamma | \Psi_{\text{GaAs}} \rangle$ to be very close to unity (better than 1 part in 10^3) for direct-gap alloys, which implies that the equality of the u 's in different layers is not as crucial an approximation as the first EFA assumption discussed above. Note that this agreement is obtained assuming the atomic orbitals are the same for both group-III atoms, respectively. Differences in the atomic orbitals, which may be relevant in other materials, lead to larger differences.

III. QUANTUM WELLS

We consider a GaAs quantum well of width W between $\text{Al}_x\text{Ga}_{1-x}\text{As}$ barriers, grown along the z direction. For the (001) x - y planes there is no quantum confinement and the carriers can move freely. In this type of quantum well (type-I) the energy difference between the larger band gap of the barriers and the smaller band gap of the well material causes a confinement potential both for the electrons in the conduction band and for the holes in the valence band.

We adopt a tight-binding supercell formalism with tetragonal cells of dimensions $N_x=N_y(=N_{||})$ and N_z . Periodic boundary conditions are imposed and for each W the value of N_z is taken sufficiently large to guarantee convergence of the calculated electronic properties to the infinitely wide $\text{Al}_x\text{Ga}_{1-x}\text{As}$ separator situations. Specific atomic configurations are generated numerically according to the occupational probabilities of the sites of the group-III sublattice: $P(\text{Al})=1-P(\text{Ga})=x$. A good description of the random atomic distribution in the (001) planes is obtained for $N_{||}=8$ ML (1 ML = 2.85 Å, i.e., half of the conventional cubic lattice constant), and for the largest W value considered here, convergence requires $N_z=70$ ML, which corresponds to cells with 4480 atoms. The tight-binding parameters were taken from Ref. 6, with the zero energy level at $E_C^\Gamma(\text{GaAs})$ (bottom of the GaAs conduction band) and a negative band offset correction to the diagonal matrix elements of AIs of $O=0.47$ eV. It should be noted that previous treatments of heterostructures using the tight-binding approximation⁹ describe the alloy region in the VCA. In this case, according to Eq. (2), the Hamiltonian matrix elements are weighted averages from the corresponding binary compounds values.

Within the EFA, the energy of the electronic conduction states (E_C) may be obtained from Eq. (1) with the attractive quantum well potential:

$$V(z) = \begin{cases} 0 & \text{for } |z| < W/2 \\ V_C & \text{for } |z| > W/2, \end{cases} \quad (6)$$

where V_C is the conduction-band offset. In Eq. (1), $m^*(z)$ is an effective mass which characterizes the different layers, and is assumed to have the same value as the corresponding bulk materials. The barrier is determined by the conduction-band minimum in $\text{Al}_x\text{Ga}_{1-x}\text{As}$. As discussed in Sec. II, this is also to be considered a Γ -symmetry point and, following the VCA scheme: $E_C^\Gamma(\text{Al}_x\text{Ga}_{1-x}\text{As}) = xE_C^\Gamma(\text{AlAs}) + (1-x)E_C^\Gamma(\text{GaAs})$. In order to compare the tight-binding results with those obtained within the EFA, we use for V_C and m^* the interpolated values obtained for these quantities from the tight-binding energy bands of the binary compounds:^{6,8}

$$V_C = x[E_C^\Gamma(\text{AlAs}) - E_C^\Gamma(\text{GaAs}) - O] = 1.02x \text{ eV}, \quad (7)$$

$$\begin{aligned} m^*(\text{Al}_x\text{Ga}_{1-x}\text{As}) &= xm_\Gamma^*(\text{AlAs}) + (1-x)m_\Gamma^*(\text{GaAs}) \\ &= (0.12 + 0.17x)m_0, \end{aligned} \quad (8)$$

where m_0 is the free electron mass. Figure 2 compares the lowest electron energy eigenvalues (E_{C1}) of the single-band envelope-function model (solid lines) with those of the tight-binding supercell method (squares), as a function of the GaAs well width when surrounded by barriers of

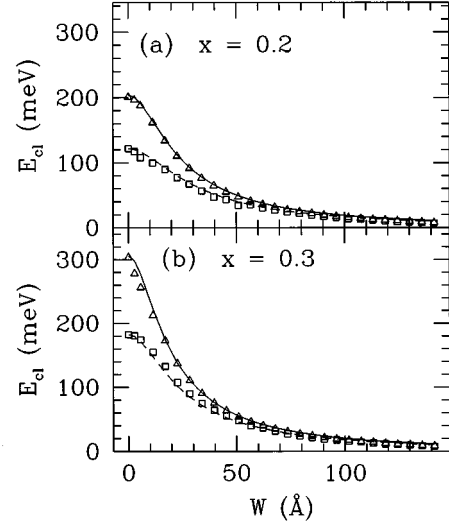


FIG. 2. Energy of the first electron state in a GaAs quantum well confined between $\text{Al}_x\text{Ga}_{1-x}\text{As}$ barriers as a function of the well width W for the indicated values of x . Results of calculations using the envelope-function approximation (solid line) are compared to the full tight-binding results (squares). Tight-binding calculations with the alloy region treated within the VCA are given by the triangles, and the dashed lines correspond to “disorder-corrected” EFA. The good agreement between the solid lines and the squares as well as between the dashed lines and the triangles indicates that the main source of discrepancy among the different approaches is the treatment of disorder in the alloy region.

$\text{Al}_x\text{Ga}_{1-x}\text{As}$ for $x=0.2$ and 0.3 . Note that each data point represents an *ensemble* average over at least five statistically generated configurations in the alloy region. Statistical error bars are smaller than the symbol size in the figure.

The energy values for $W=0$ represent V_C , which is well above the tight-binding energy for the compositions considered. For narrow wells the tight-binding results for the energy are consistently lower than the envelope-function ones, differing by about 80 meV for widths of 2 ML for $x=0.2$, and by about 100 meV for $x=0.3$ (see Fig. 2). As W increases, the results from both methods approach, and they converge faster for the larger x . For $x=0.2$, agreement within 5 meV is obtained only for well widths W above 80 Å, while a similar agreement for $x=0.3$ is already achieved for $W=60$ Å. So, as x increases, the narrow well region difference in energy increases while in the wide W region the agreement between the EFA and tight-binding results improves. This apparently contradictory result is attributed to the difference of barriers height in the two cases. The barrier height increases with x . As illustrated in Fig. 3 for $W=40$ Å, the wave function is more localized in the well (GaAs) region for $x=0.3$ than for $x=0.2$. Therefore the effects of disorder in the alloy region become less relevant as x increases. From Fig. 3 we also note that the wave functions for EFA are more localized in the well than the tight-binding ones. Another indication of this localization effect is the narrower superlattices miniband widths obtained in the EFA. For a 34 Å(GaAs)/17 Å($\text{Al}_x\text{Ga}_{1-x}\text{As}$) superlattice with $x=0.3$, the bandwidth calculated within the EFA is 42 meV, while the tight-binding result is 50 meV.

We now show that, among the approximations underlying

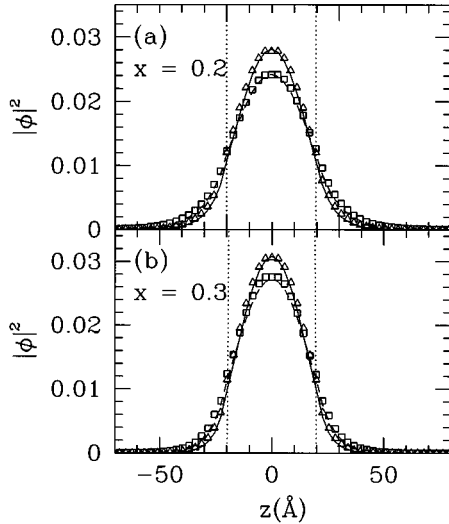


FIG. 3. Envelope function squared of the first electron state in a GaAs quantum well confined between $\text{Al}_x\text{Ga}_{1-x}\text{As}$ barriers for well width $W=40$ Å and for the indicated values of x . Interface positions correspond to the vertical dotted lines. Different approaches correspond to the same symbols and lines given in Fig. 2.

the envelope-function approach, treating of the alloy disorder within the VCA is responsible for the quantitative discrepancy obtained in the narrow well limit. Two combined calculation schemes are adopted. First, we perform tight-binding calculations with the alloy region treated within the VCA and the results, given by the triangles in Figs. 2 and 3, agree with the EFA/VCA (solid lines) essentially over the whole range of W values. The second scheme is a “disorder-corrected” EFA. Barriers described within the VCA lead to higher energies, i.e., states more localized in the well region than when different atomic species are considered in the alloy region. This indicates that the VCA produces effectively higher barriers for the alloy than the actual disordered atomic potential. In practice it is possible to compensate for this effect by lowering V_C to agree with the full tight-binding calculation value. For the composition range $0 < x < 0.3$, the full tight-binding calculation yields $V_C^{\text{TB}} = 0.61x$ eV, which means the linear x dependence in Eq. (7) is preserved but VCA overestimates the barrier height by over 60%. Using V_C^{TB} instead of V_C in Eq. (6), the EFA yields the results given by the dashed lines in Figs. 2 and 3. The agreement between the EFA and the full tight-binding results (dashed lines and squares in the figures) improves to cover the whole range of W . The two combined schemes demonstrate that tight-binding and EFA approximations lead to essentially the same results when disorder effects are taken into account consistently. However, using V_C^{TB} in the miniband widths calculations usually leads to wider bands than obtained in the full tight-binding approach. In the example given above, the “corrected” EFA yields 58 meV wide minibands, i.e., 8 meV above the full tight-binding result, while using V_C given by Eq. (7) leads to a value that is narrower by the same amount, as given above.

Corrections due to disorder in the effective mass expression (8) are harder to define since m^* is related to the energy variation with \vec{k} . When disorder is taken into account realis-

tically, \vec{k} is not a good quantum number. In our supercell calculations, it is possible to introduce a \vec{k} Bloch wave vector associated with the supercell periodicity. Effective masses so calculated in a supercell with 216 atoms differ from those given in Eq. (8) by no more than $0.01 m_0$. EFA model calculations performed with these modified values yield essentially the same results and trends presented above.

IV. DISCUSSIONS AND CONCLUSIONS

We have investigated the validity and limitations of the EFA, especially with respect to the treatment of atomic-scale effects in the potential. Concerning the nature of the band-edge wave functions in bulk $\text{Al}_x\text{Ga}_{1-x}\text{As}$, our results suggest that the symmetry of the wave functions is qualitatively preserved in these disordered alloys, as long as x is not close to x_c .

The tight-binding supercell approach for describing the energy spectrum and wave functions of the first electron state in narrow quantum wells clearly indicates that, for the materials investigated here, the EFA/VCA is valid only for well widths above ~ 50 Å. This is well within the validity assumptions stated by the EFA.¹ The discrepancy between the theories increases for decreasing well width. We have demonstrated that this is due to a steady decrease of applicability of the VCA in the alloy barrier of narrow quantum well structures as the wave functions penetrate more into the barrier region.

The breakdown of the EFA in narrow quantum wells has been recently investigated by Long *et al.*⁴ by considering CdTe wells between $\text{Cd}_{1-x}\text{Mn}_x\text{Te}$ barriers. There, the EFA energies are compared to pseudopotential results, which take into account the atomic-scale nature of the potential. The alloy region in the pseudopotential calculations is also treated within the VCA.¹⁰ The discrepancies obtained there are thus of a similar nature as obtained here in Fig. 2 by comparison of the EFA (solid line) and the tight-binding VCA (triangles). Several approximations in the EFA are responsible for this effect, as, for example the Bloch functions description discussed in Sec. II, the effective mass approximation,¹⁰ and the matching conditions for the envelope function across the interfaces.^{2,3} We have not investigated those separately, and in agreement with Long *et al.*,⁴ the EFA yields somewhat higher energies than the microscopic potential calculations, even when the alloy region is treated within the VCA. From the results presented in Fig. 2, we conclude that corrections due to alloy disorder effects in the barrier region are far more relevant than those implied by the other EFA assumptions. Therefore, treating the alloy region within the VCA is a severe limitation in either effective-medium or microscopic potential calculations.

We have shown that, within the EFA, it is possible to correct for the treatment of alloy disorder effects by lowering the well height. This leads to very good estimates for the electronic energy eigenstates even for narrow wells. It should be noted that reliable values for the EFA input parameters are not always available for different alloys, and that they are frequently interpolated from the (binary) compound values, following the VCA. Our results indicate that linear interpolation schemes are particularly inadequate for narrow quantum wells, and that experimentally determined parameters,

when available, should definitely be used instead of VCA interpolations. On the other hand, lower barriers lead to wider minibands in superlattices. Notice that superlattices involve multiple heterointerfaces. Also, the wave function penetration in the alloy barriers region is always relevant. Therefore enhanced discrepancies due to *all* EFA approximations are expected in superlattices in comparison with a single quantum well. Adopting a value for the barrier height that fits experiment for the bulk alloys or for isolated quantum well levels does not necessarily lead to accurate estimates of the miniband widths. It was observed by Voisin¹¹ that experimentally measured miniband widths are typically $\sim 30\%$ smaller than those calculated within standard EFA. A possible explanation for this discrepancy is the value for the barrier height adopted in the EFA calculations.

The calculations reported here refer to the simplest model of heterostructure levels and materials where the EFA has

been successful. Disorder and size effects are shown to affect the reliability of the results in different situations, and these effects are expected to persist in a qualitatively equivalent way even in more complex models.

ACKNOWLEDGMENTS

We thank P. Voisin for calling our attention to the miniband widths problem. This work was partially supported by the Brazilian agencies Conselho Nacional de Desenvolvimento Científico e Tecnológico (CNPq), Financiadora de Estudos e Projetos (FINEP), Fundação de Amparo à Pesquisa do Estado do Rio de Janeiro (FAPERJ), and Fundação Universitária José Bonifácio (FUJB). The use of computational facilities at Núcleo de Atendimento em Computação de Alto Desempenho (NACAD-COPPE/UFRJ) is also acknowledged.

¹G. Bastard, *Wave Mechanics Applied to Semiconductor Heterostructures* (Les editions de Physique, Paris, 1988); G. Bastard, J. A. Brum, and R. Ferreira, *Solid State Physics: Advances in Research and Applications*, edited by D. Turnbull and H. Ehrenreich (Academic, New York, 1991), Vol. 44, p. 229.

²D. J. Ben Daniel and C. B. Duke, *Phys. Rev.* **152**, 683 (1966).

³M. G. Burt, *J. Phys.: Condens. Matter* **4**, 6651 (1992); W.A. Harrison and A. Kozlov, in *21st International Conference on the Physics of Semiconductors*, edited by P. Jiang and H.-Z. Zheng (World Scientific, Singapore, 1992), p. 341.

⁴F. Long, W. E. Hagston, and P. Harrison, in *23rd International Conference on the Physics of Semiconductors*, edited by M. Sheffler and R. Zimmermann (World Scientific, Singapore, 1996) p. 819.

⁵B. Koiller and R. B. Capaz, *Phys. Rev. Lett.* **74**, 769 (1995).

⁶P. Vogl, H. P. Hjalmarson, and J. D. Dow, *J. Phys. Chem. Solids* **44**, 365 (1983).

⁷The order parameter was conveniently chosen to be the dipole moment squared of the optical transition between band edges. When properly normalized, this quantity varies from 1 (order) for direct-gap GaAs to 0 (disorder) for indirect-gap AlAs.

⁸Although these values differ from the experimentally determined ones, they are used to assure consistency in the comparisons.

⁹S. Vlaev, V. R. Velasco, and F. García-Moliner, *Phys. Rev. B* **50**, 4577 (1994).

¹⁰F. Long, P. Harrison, and W. E. Hagston, *J. Appl. Phys.* **79**, 6939 (1996).

¹¹P. Voisin, in *Wannier Quantization in Semiconductor Superlattices*, edited by Jan Kaczer, Trends in Physics (Prometheus, Prague, 1991), p. 692; (private communications).